High-yield prebiotic polymerization of 2',3'-cyclic nucleotides under wet-dry cycling

Federico Caimi[1,*], Juliette Langlais[2,*], Francesco Fontana[1,*], Sreekar Wunnava[2], Tommaso Bellini[1,°], Dieter Braun[2,°] & Tommaso P. Fraccia[1,°]

* Joint first authors; ° Joint corresponding authors;
tommaso.bellini@unimi.it, dieter.braun@lmu.de, tommaso.fraccia@unimi.it

[1] Dep. of Medical Biotechnologies and Translational Medicine, University of Milan, via Fratelli Cervi 93, I-20090 Segrate, Milano, Italy
[2] Systems Biophysics, Ludwig-Maximilians-University Munich, Amalienstr. 54, 80799 Munich, Germany
[3] Dep. of Pharmacological and Biomolecular Sciences, University of Milan, via Balzaretti 9, I-20133 Milano, Italy

Abstract

The spontaneous formation of RNA polymers is one of the most crucial yet unsolved steps in the investigation of the origin of life. RNA oligomerization from nucleotide solutions has so far been reported only with low reactivity. Here we show that 2',3'-cyclic nucleotides of all four nucleobases efficiently polymerize without external activators when dehydrated at room temperature in a mild alkaline pH range. Oligomerization yield, Y, and the polymer length further increase by wet-dry cycling, peaking at Y ≈ 70% in guanosine solutions and Y ≥ 20% for the other nucleobases when individually solubilized. Microscopy observation during drying indicates that the guanosine reactivity is enhanced over the other nucleobases by its self-assembly propensity. We show that at pH 11, a condition disfavoring guanosine structuring, polymerization in stoichiometrically balanced solution of the four nucleotides reaches Y = 36% and well distributed inclusion of nucleobases in the chains. The simplicity of the procedure, where only water is added at each cycle, makes this process a promising candidate for the prebiotic origin of RNA oligomers on early Earth.

Keywords: abiotic RNA polymerization, origin of life, nucleotides self-assembly, dry-wet cycles

INTRODUCTION

It's widely accepted that RNA is a fundamental molecule for the origin of life [1,2]. However, the prebiotic emergence of polymeric RNA is still an unsolved question. RNA polymerization from single nucleotides poses significant challenges, being extremely inefficient in water, due to the predominance of hydrolysis over condensation [3,4]. The use of activated nucleotides, such as 5'-phosphorimidazolides, on the surface of clays, such as montmorillonite [5], or in presence of prebiotically improbable ions, such as Pb^{2+} and Zn^{2+} [6,7], partially mitigated the problem. Only 5'-phosphorimidazolides of adenosine (5'-ImpA) have been reported to polymerize efficiently enough, with a maximum conversion yield of 61% in presence of montmorillonite after 3 days (10 nt max length) [5], or 25% in presence of Zn^{2+} after 10 days (4 nt max length) [6], or 50% in presence of Pb^{2+} after 7 days (5 nt max length) [7]. While the availability of such activated nucleotides on early Earth is still to be demonstrated, a more intriguing alternative is provided by 2',3'-cyclic phosphate nucleotides (cNMPs) (**Fig. 1a**) since their prebiotic synthesis has been shown to be plausible [8,9] and because cyclic 2',3'-phosphate is the natural product of RNA phosphodiester bonds cleavage [10].

Amine catalyzed polymerization of 2',3'-cAMP has been reported to reach 69% yield for 3 days dry state incubation at room temperature and in presence of 1,2-diaminoethane at pH 9.5 [11,12]. This finding was recently extended by the observation of the formation of oligomers of all four 2',3'-cNMPs as a result of sample drying at mild alkaline pH at high (40 – 80°C) [13] or room temperature (RT) [14]. The reaction is described to proceed via general acid-base catalysis (**Fig. 1b**), with optimal reactivity observed at pH 10. Generally, low reaction yields (<0.1% at 40°C and < 2% at RT) were observed except for cGMP (~3.5% at 40°C and ~15% at RT), which has a much larger reactivity, yielding to its preferential inclusion in the resulting oligomers at the expense of other nucleobases [13,14]. This phenomenon appears problematic in the context of the emergence of catalytic activity in the early Earth, which requires a large degree of sequence heterogeneity driving RNA hybridization, secondary structuring and assembly. Added hydrophobic amino acids, such as Valine, has been recently reported to act as catalysts, enhancing the reactivity at room temperature (35% for G and ~7% for A, U and C) and the compositional diversity of the emerging oligomers [14].

In this study, we report unpreceded high-yield polymerization of all four cNMPs via dehydration-rehydration cycles (**Fig. 1c,e**) performed without the addition of any external activator at room temperature and mild alkaline conditions. We found that the combination of low enough temperatures, slow evaporation (8 to 10 hours, see **methods**) and dehydration-rehydration cycles significantly enhanced both the yield, the length distribution and the compositional diversity of the resulting RNA oligomers. This is exemplified in **Fig. 1d** where we show a HPLC chromatogram of the mixture of all the four nucleotides after 10 cycles, revealing the emergence of distinct peaks at larger retention times that correspond to high-yield production of RNA oligomers up to at least 10 nucleotides long. Analyses were strengthened by HPLC-MS, enabling the detailed attribution of each HPLC peak (**Fig. 1d**, **inset** and **SI methods**). Cycles were produced by adding pure water (no ions or buffers), a choice meant to mimic the behavior of ponds subjected to evaporation and rehydration processes by natural cycles such as day-night, rains, tidal and seasonal successions. Dry-wet cycles have been shown to play fundamental roles in origin of life scenarios, driving building blocks synthesis, polymerization by condensation and compartments assembly [15–23].

All experiments reported here started with 50 mM reactants, unstructured, isotropic, aqueous solutions (blue shading in the sketches of **Fig. 1c,e** and **methods**). During dehydration, as the concentration of cNMPs increases, some of the samples become structured either when in state of concentrated solutions (green shading) or when dehydrated solids (orange shading). This is certainly the case of samples of guanosines that are expected to self-assemble in columns of planar

hydrogen-bonded guanosine quartets (G-quartets) that can in turn collectively organize into liquid crystal and crystalline structures [24–26]. The presence of such forms of anisotropic molecular ordering made the samples locally birefringent, a property that was readily detected via polarized transmitted optical microscopy (PTOM), which was routinely performed to characterize the samples during wet-dry cycles. This analysis enabled us to evaluate the interplay of physical molecular ordering and the chemical polymerization process.

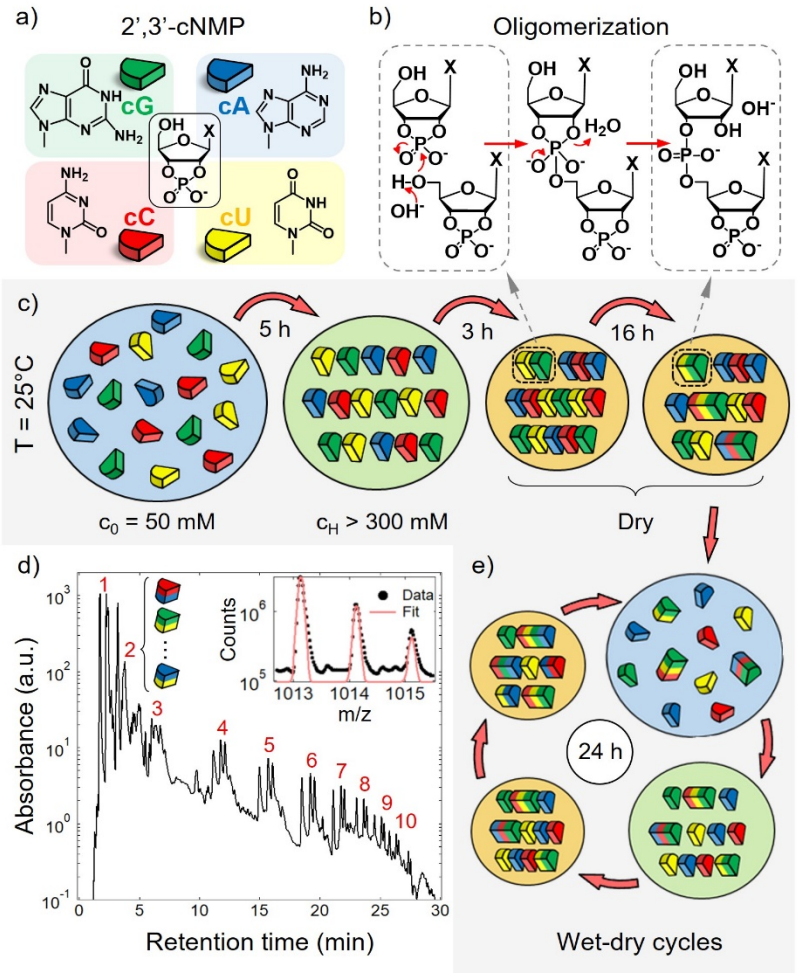

Figure 1 – ***Polymerization by dry-wet cycling of 2',3'-cyclic phosphate nucleotides.***
a) Molecular structures and sketches of the four canonical 2',3'-cyclic phosphate nucleotides (2',3'-cNMPs) studied in this work.
b) Reaction scheme of the base-catalyzed transesterification leading to the formation of phosphodiester bonds of RNA oligomers.
c) Schematic illustration of the evaporation process of an aqueous solution (blue) containing a 2',3'-cNMP mixture of all the four different nucleotides at room temperature. During drying, depending on pH and nucleotide species, the solution may enter a regime of supramolecular organization at sufficiently large concentration, c_H (green). In fully dry condition (orange), oligomerization proceeds by transesterification as depicted in panel b.
d) HPLC-MS chromatogram (log scale) of the oligomerization products in AUGC mixture (pH = 10) after 10 wet-dry cycles. The groups of peaks corresponding to oligomers with the same length ≤ 10 nucleotides are labeled in red. Inset: Section of the MS spectrum overlaying the isotope distribution of the polymerization product GGU-2'/3'p in the z = 1 charge state. The fit is used for the quantification of the product.
e) Wet-dry cycles are implemented by new additions of pure water to the dry state with a period of t = 24 hours.

RESULTS AND DISCUSSION

Polymerization of 2',3'-cyclic NMPs at mildly alkaline pH in single drying processes

Oligomerization experiments were performed on solutions comprising single 2',3'-cNMP (N = A, U, G, C) species, binary Watson-Crick pairs (AU and GC) and mixtures of all four nucleotides (AUGC). Aqueous solutions with initial total cNMP concentration c_0 = 50 mM were evaporated over 24 hours at room temperature. Potassium hydroxide (KOH) was used to set the initial pH at values ranging from pH 6 to 12, unless specified otherwise (**methods**). The HPCL, HPLC-MS and PTOM results we obtained from a single drying process are summarized in **Fig. 2**.

The oligomerization yields strongly depended on both the nucleobase and pH (**Fig. 2a,b and S1, 2**). All nucleotides and mixtures exhibited only negligible oligomerization at pH 6, while the reaction efficiency increases at alkaline pH values. This behavior was consistent with previous observations performed at higher temperature [13] or in presence of amino acids [14], further confirming that the polymerization of cNMP follows a general basic catalysis mechanism. In this process, a basic moiety deprotonates the 5'-hydroxyl group of a nucleotide, increasing its nucleophilicity and facilitating its attack on the 2',3'-cyclic phosphate of a second nucleotide. The resulting intermediate then decays, leading to the formation of either a 3'-5' or 2'-5' phosphodiester bond between the two nucleotides, with the proton being accepted by the conjugate acid of the base or by the hydroxyl group of a third nucleotide (**Fig. 1b**). While the analytical tools adopted here do not enable distinguishing 3'-5' from 2'-5' linkages, previous studies on similar systems reported an approximate 1:1 ratio between the two [13,14]. It was also shown that backbone heterogeneity does not hamper RNA folding into functional 3D tertiary structures [27], making the two forms equally relevant for the appearance of ribozymes in the prebiotic world.

The reactivities reported in **Fig. 2a,b** are markedly larger than the ones previously reported in literature, a difference we attributed to the lower temperature and slower drying, possibly favoring supramolecular interactions. The oligomerization yield, Y, of cGMP is the highest among all single nucleotides, reaching 65% at pH 10, followed by cCMP (28% at pH 11), cAMP (17% at pH 10), and cUMP, which increased steadily with pH, up to 19% at pH 12. While G showed the highest reactivity across all pH levels, the relative reactivity of the other bases varied with pH: A > C > U at pH 10, C > A ≈ U at pH 11, and U > A ≈ C at pH 12.

Fig. 2c shows the HPLC-MS analysis of the length distribution c_L of the products, expressed as molar concentration of the oligomers. From preparations in the millimolar range – a prebiotically acceptable monomer concentration [23,28] – we found at least 4-base-long homo-oligomers of all four nucleotides with concentrations ranging from 100 µM to 1 mM, and homo-guanosine 10-mers at 20 µM. We found the length distribution c_L to generally deviate from the simple exponential decay, expected for step-growth linear polymerization [29], to slightly favor longer products [30] (**Fig. S3**). This behavior was particularly evident for G (**Fig. S3 and S4**). For example, the polymerization of G at pH 8 generated longer products than at pH 12 despite similar Y. Similarly, C at pH 11 gave longer products than U at pH 12 and U at pH 11 gave longer products than C at pH 12. Generally, while alkaline pH is necessary to boost reactivity, a large excess of OH^- lead to shorter products.

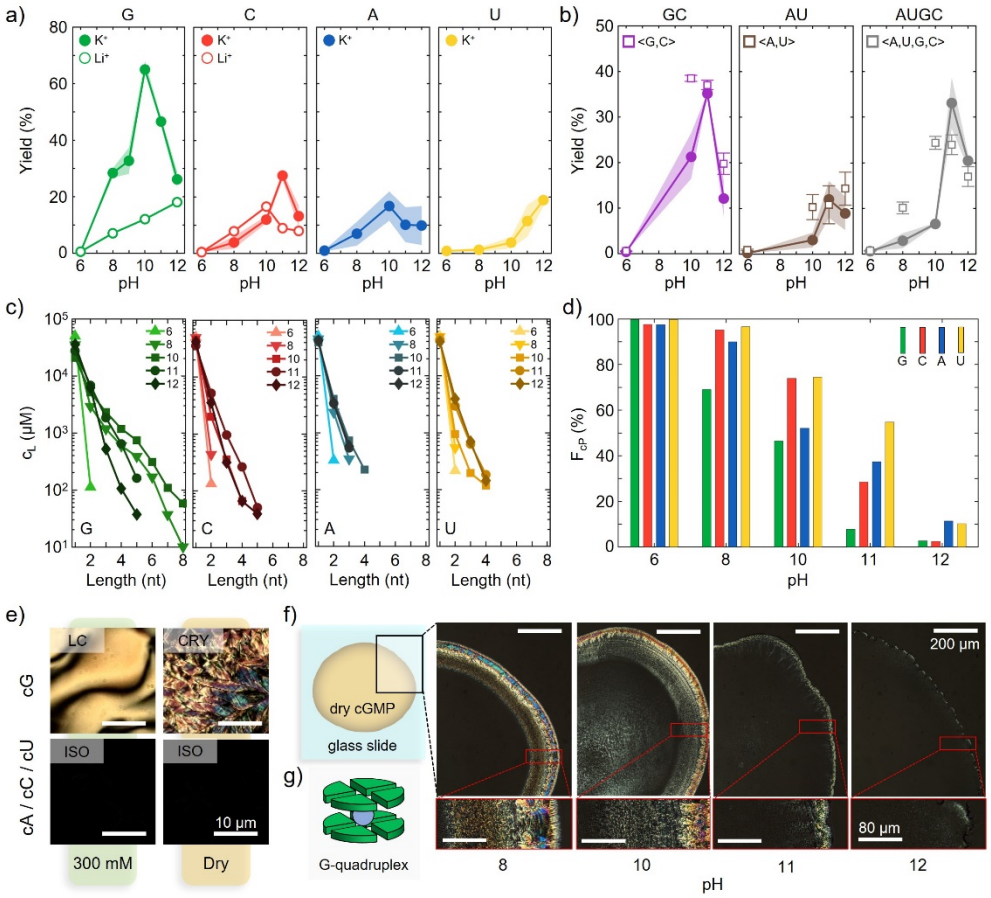

Figure 2. Polymerization of 2',3'-cNMP after a single dehydration at mildly alkaline pH.
a,b) *Polymerization yields as a function of the initial pH for solutions of (a) individual 2',3'-cNMP species at a total concentration of 50 mM and (b) binary and quaternary mixtures after 24 hours drying at room temperature. Data are obtained by averaging HPLC and HPLC-MS measurement and colored shading marks the confidence interval (SI methods).* ***c)*** *Length distribution of the formed RNA oligomers as a function of pH.* ***d)*** *Fraction of cyclic terminal phosphates F_{cP} over the total amount of molecules after the reaction, calculated considering monomers and oligomers at the same time.* ***e)*** *Polarized transmitted optical microscopy (PTOM) images of 2',3'-cNMP solutions during evaporation at pH 10, in concentrated (left) and dry (right) state, showing the formation of liquid crystal and crystal phases only in presence of 2',3'-cGMP.* ***f)*** *PTOM images of the dry state of 2',3'-cGMP droplets showing a reduction of the birefringent crystalline domains at increasing pH.*

To better understand the pH dependence of the reaction mechanism, we measured by HPLC-MS the amount of hydrolyzed and unreacted 2',3'-cyclic phosphates after the reaction. **Fig. 2d** shows the fraction F_{cP} of the terminal phosphates for monomers and oligomers that have remained in the cyclic form and are thus potentially reactive. In other words, F_{cP} expresses the fraction of 2',3'-cyclic phosphates that have not been hydrolyzed, confirming that a strong alkaline environment favors the opening of the 2',3'-cyclic to either 2' or 3' linear phosphates (**Fig. S5**). Thus, cyclic phosphate opening, which is the necessary starting step toward polymerization, is also responsible for the reduced availability of reacting species. The combination of these opposing elements - cyclic phosphate opening, inter-nucleotide phosphodiester bond formation and phosphodiester bond hydrolysis - lead to an optimal condition for oligomerization which appeared to be around pH 10 – 11 for almost all nucleotides and mixtures, U being the relevant exception which is more tolerant to higher pH. During evaporation the initial pH evolution depended on the nucleobases (**Fig. S6**). In fact, guanine and uridine have self-buffering capability toward alkaline conditions because of the pKa of their nitrogen atoms (N1 in G and N3 in U), allowing each RNA base to stabilize the pH in the

drying process. Data however suggests that, despite pH drifts in different ways depending on the base, the resulting oligomerization largely depends on the initial pH.

In **Fig. 2b** we compared, for different pH values, the yield of AU, GC and AUGC mixtures with the average yields of the respective single nucleotide solutions (open squares). While in general mixing appeared to reduce the yields with respect to the individual nucleobase systems, at pH 11 instead the yield for AU and GC mixtures matched the one expected from the average of their components and was even larger for the case of AUGC mixtures (33% at pH 11). These observations suggest that pH can tune the nucleobase composition of heterogeneous nucleobase polymerization as discussed in detail later.

To determine the stage of evaporation at which the reaction took place, we performed HPLC analysis of products at different times, t, during dehydration. We found no relevant oligomerization in the liquid state, nor in the denser LC phase, even by stopping the evaporation to incubate the samples in these conditions for several hours (**SI Fig. S12**). For each nucleotide, we detected reaction products only after the dry state was achieved. Kinetics assays in the dry state indicated that for all bases the polymerization yield over time, Y(t), followed an exponential growth with characteristic times shorter than 24 hours, specifically, τ = 0.7, 2.8, 3.5 and 6.9 hours for G, A, C, U respectively at pH 11 (**SI Fig. S12**).

Effects of supramolecular assembly during drying

Fig. 2a,c shows that the polymerization capability of G is much larger than that of all other nucleobases. It was suggested that the enhanced activity of G is in part due to the pKa = 9.3 of the N1 nitrogen [31] which may assist the acid-base catalysis at alkaline pH [14]. There is however another element that could play a role, which is the peculiar self-assembly propensity of G nucleotides. Solutions of 5'-GMP, 3'-GMP, 2'-GMP and 3',5'-cyclic phosphate GMP, as well as their deoxyribose analogs 3'-dGMP, 5'-dGMP and cyclic 3',5-dGMP, have been found to self-assemble in G-quartets, planar structures formed by four mutually hydrogen bonded guanosines, in which N1 and N2 on the Hoogsteen hedge act as hydrogen bond donors while N7 and O on the Watson-Crick hedge act as acceptors [24,26]. G-quartets, in turn, stack into linear columnar structures (G-quadruplexes, **Fig. 2g**) that, at large enough concentrations, develop collective ordering into liquid crystal (LC) lyotropic chromonic phases [26,32,33]. 2',3'-cGMP was not considered in those previous studies.

Since the LC ordering gives rise to a significant optical anisotropy, we performed systematic PTOM observations on all our samples before, during and after drying (**SI Fig. S7-10**). We found that, as the 2',3'-cGMP concentration overcomes 300 mM, birefringent domains nucleated and grew to fill the whole sample with the smooth birefringent textures typical of nematic LC phases, as shown in **Fig. 2e** (top-left panel). Upon further drying, the uniformity was lost and replaced by a faceted structure (top-right panel), indicating that birefringence, and thus long-range molecular ordering, was retained but on a smaller scale, suggesting poly-crystallinity (CRY). In our experiments, as far as PTOM observations, 2',3'-cGMP behaved very similarly to 5'-GMP.

On the contrary, no birefringence-signals of collective ordering were found in solutions of A, U, C, which exhibit featureless dark PTOM images throughout the drying process (**Fig. 2e** bottom panels and **S10**), indicating a transition from an isotropic fluid to a transparent amorphous glassy state, independently of the pH. At higher pH, only the appearance of sharp-edged KOH crystals was detected. Since LC phases were previously found in binary mixtures of deoxynucleotides triphosphates [33], we searched for analogous structures in cyclic nucleotides mixtures, which

instead we could not detect: AU mixtures showed no birefringence while GC and AUGC mixtures exhibited only insulated birefringent domains, conceivably produced by G-quadruplexes assemblies coexisting with isotropic glass regions (**SI Fig. S11**).

On this basis, it is conceivable that the large reactivity of G is at least partly due to supramolecular ordering by which the reacting moieties are held in continuous proximity, in analogy with the proper positioning of the reacting species provided by enzymes. Indeed, LC ordering was demonstrated effective in templating non-enzymatic ligation of oligomeric DNA and RNA duplexes [34,35], but was not reported in systems of nucleotides. At high pH [36], G-quartets assembly becomes disfavored due to the deprotonation of the N1 nitrogen [31] involved in the hydrogen bonds responsible for the assembly of G-quartets [37]. The disruption of molecular ordering can be appreciated in the PTOM observation of droplets of same size and same nucleotide concentration at various pH after full dehydration, reported in **Fig. 2f**. This observation suggests that the peak of the reactivity of G at pH 10 may result from the combination of the appropriate phosphate opening chemistry, favored at high pH, and the geometrical arrangement provided by G-quadruplexes, favored at neutral pH. This notion is also supported by the shape of c_L, which at pH 8 and pH 10 is clearly bimodal (**Fig. S4**), while at larger pH, where the self-assembly is disrupted, becomes similar to the one of the other nucleotides (**Fig. S3**).

An alternative mean to disrupt G-quadruplexes is to replace counterions with Li^+ ions (**methods**) [38,39], whose size is much smaller than the cavities inside the G-quadruplex structure (blue sphere in the sketch of **Fig. 2g**) that are thus destabilized. In these conditions, the reaction yields of cGMP sharply decreased (open dots in **Fig. 2a**) and became comparable with those of the other nucleotides. By contrast, the same ions replacement didn't significantly modify the reactivity of cCMP. These observations further confirm the notion that molecular assembly plays a role of no less importance than pH in regulating the reactivity of 2'3'-cGMPs under the given conditions and suggest an approach to decrease reactivity mismatches between nucleobases, i.e., destabilize G self-assembly.

Enhanced polymerization yield by dry-wet cycles

Although prolonging the incubation in the dry state for $t >> \tau$ did not significantly impact the polymerization yield of single nucleotide systems (**SI Fig. S12**), a relevant amount of potentially reactive 2',3'-cyclic phosphate termini were still available after 24 hour, either from initial 2',3'-cNMPs monomers or at the terminal of the produced oligomers (**Fig. 2d and S5**), suggesting that cyclic phosphates are blocked by dehydration into positions hindering their reaction. Prompted by this observation, we periodically rehydrated and dehydrated the samples in wet-dry cycles to explore whether in a "reshuffled" dry state the remaining 2',3'-cyclic phosphate groups could react. We performed a series of up to 10 cycles at Δt = 24 hours intervals. On each cycle only pure water was added to recover the initial nucleotide and salt concentration and a small fraction was collected for pH measurement and products analysis with HPLC and HPLC-MS (**methods**).

Fig. 3a,b show the oligomerization yield as a function of the number of cycles, n, in single nucleotide solutions and in mixtures at pH ≥ 10. In all cases except for G at pH 12, Y(n) initially grew, Y(2) > Y(1). Further cycling led to various behavior: growth of Y, saturation or decrease depending on the system and on pH. The initially less reactive nucleotides (cCMP, cAMP and cUMP) were found to benefit from cycling, showing a maximum yield of 33% for A at n = 7 and pH 10, and Y = 32% and Y = 25% for C and U, respectively, achieved at n = 5 and pH 11 (see also **Fig. S13**). These nucleotides strongly benefitted from the reshuffling of their positions in the dry state, an occurrence that can take place only by fluidizing the system again by a successive hydration step. By contrast,

the growth of the yield of G after the first cycle at pH ≥ 10 was limited, a behavior that we understand as a consequence of a polymerization already very effective in the first evaporation, leaving little reactants for further improvement (**Fig. S13**).

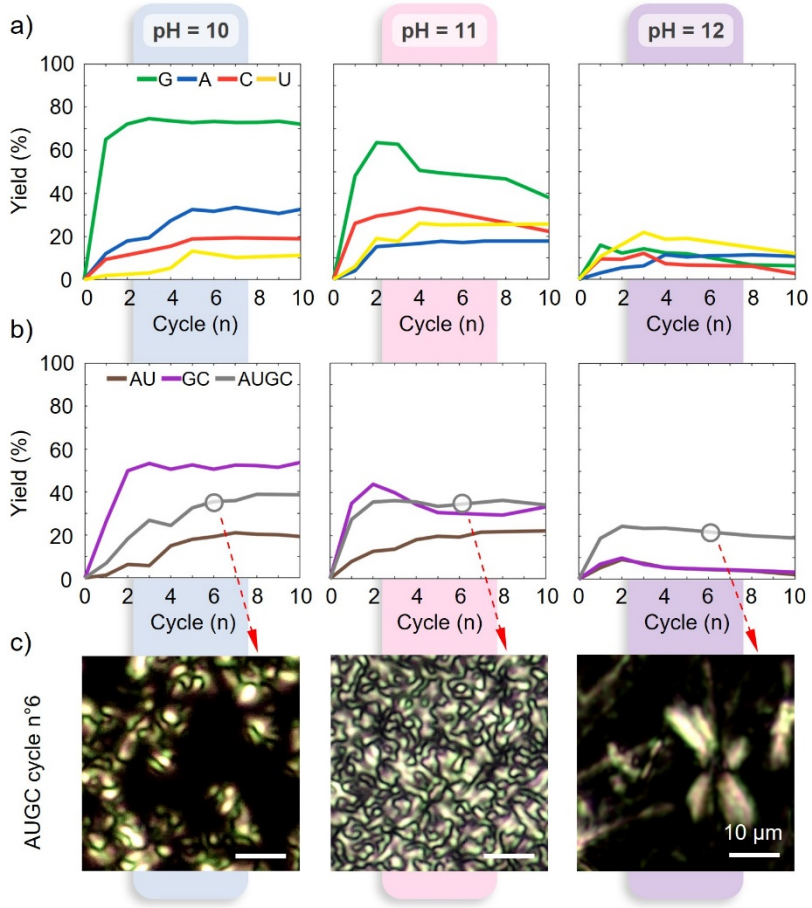

Figure 3. Enhanced polymerization by dry-wet cycles.
a) Polymerization yield as a function of the number of cycles for 2',3'-cNMP solutions at pH 10 (left panel), pH 11 (central panel) and pH 12 (right panel). b) Polymerization yield as a function of the number of cycles for 2',3'-cNMP mixtures at pH 10 (left panel), pH 11 (central panel) and pH 12 (right panel). c) PTOM images of AUGC mixtures showing different birefringent domains geometries. Images were acquired after the 6th cycle in three samples with different initial conditions: pH 10 (left panel), pH 11 (central panel) and pH 12 (right panel). Yield values were obtained from HPLC analysis (methods).

Upon rehydration cycles, we measured decreasing values of pH that converged to a constant value at n ~ 6 for all cNMPs solutions. The average drop was ~2 pH units, with maximum drop being 4 pH values for solutions prepared at initial pH 10 (**Fig. S14**). Such behavior indicated an acidification by the combined effect of 2',3'-phosphate ring opening (**Fig. S13**) and incorporation of CO_2 from the environment. We found that the evolution of Y(n) upon wet-dry cycling strongly depended on the initial pH. While cycling at initial pH 10 led to an increase or saturation of Y(n), experiments performed at larger pH led in some cases to a decreasing Y(n). The decrease of Y(n) was also evident when experiments were performed by adjusting the pH at every cycle around the optimal reactivity value that was found in cycle 1 (**Fig. S15**). We understand this behavior as a progressive degradation of the reactive cyclic phosphates and of the produced oligomers via hydrolysis (**Fig. S13**), the latter appearing more severe for poly-G chains.

Cycling had a strong effect on the oligomerization of binary and quaternary mixtures (**Fig. 3b)**, which reached a maximum yield of 53% for GC at pH 10, 22% for AU at pH 10 and 36% for AUGC at pH 11. With increasing n, the yield of the mixtures was found to generally approach the average of the yield of the relative single nucleotides systems (**SI Fig. S16**) with the only exception AU at pH 12. Moreover, the yield of the AUGC mixture at pH ≥ 11 overcome that of CG and AU mixtures and of their averages (**Fig. 3b** and **S16**), suggesting that in these conditions heterogeneous polymerization is larger than the homogeneous one.

Enhanced nucleobase heterogeneity by dry-wet cycles

A basic requirement for the RNA world is the production of chains with the significant degree of heterogeneity in their nucleobase sequence that is required to promote sequence elongation [35,40] and replication [41,42] through base pairing and non-enzymatic ligation. Thus, for the spontaneous polymerization of 2',3'-cNMPs by wet-dry cycling to be a source of building blocks of longer chains, it needs to offer a large palette of nucleobase alternation along the chain. Our results show that, if not mitigated via alkaline conditions, the larger reactivity of G might lead to G-dominated oligomers [13,14], in which the strong association of the G-rich sections would hinder the access to secondary structures based on Watson-Crick pairing. A balanced incorporation of the different nucleobases in the produced RNA oligomers would likely require at least two conditions to be met: equalizing the reactivity of all four nucleotides, and granting homogeneous spatial distribution of the reactants to ensure equal probability of contacts among different species.

Our data suggest that these conditions can be achieved at pH ≥ 11 and increasing n, where the polymerization yields of individual A, U, G and C become similar (**Fig. 3a and SI Fig. S17**). At the same time, PTOM observations of the dry state of AUGC mixtures revealed that the self-assembly capability of the system is also modified during dry-wet cycles, driving the formation of different morphologies (e.g., at n = 6, **Fig. 3c**). Indeed, at pH 10 we observed coexistence of crystals and amorphous glass, which we understand as a phase separation between a G-rich crystal phase and other nucleotide species. This interpretation agrees with the observation of a similar coexistence in GC mixtures, in the same conditions, while only isotropic amorphous glass phase is observed in AU mixtures or in absence of G (**SI Fig. S10,11,18**). Conversely, at pH 11 much more homogeneous crystalline phases are observed throughout the whole sample, suggesting a form of ordering in which all polymerization products participate (**SI Fig. S18**).

To probe whether the combination of equalized reactivity of different nucleotides and a homogeneous dry state can influence the degree of chain heterogeneity, we analyzed by HPLC-MS the nucleobase composition of the RNA oligomers produced after 1 and 10 wet-dry cycles of cNMPs mixtures, with initial pH = 6 – 12 (**Fig. 4**, **SI Fig. S19-25** and **SI methods)**.

AU mixtures were characterized by similar polymerization yields of individual A and U systems, for pH ≥ 11 (**Fig. 3a** and **S17**), and by homogeneous isotropic amorphous glass dried states, at each pH (**Fig. S18**). **Fig. 4a** shows the concentration, c, of each combination of A and U in chains of length 2 – 5 at pH 10 and pH 11. In this analysis, the ordering of the sequences cannot be distinguished by the mass spectrometry, e.g. "AAU" ≡ {AAU, AUA, UAA}. c is expressed in terms of the original concentration, i.e. 50 mM of nucleotides. The results are compared with the expected product distribution for random polymerization (RP) based on the combinatorics of reshuffled RNA sequences with the same length (black line) with the total concentration equal to the sum of the measured concentrations of the given N-mers at cycle 10 (see **SI methods** and **Fig. S22**). At pH 11 we found a good agreement between the measured c and the distribution expected for random polymerization, with the only exception of UUUU excess (see also **Fig. S25**). This result indicates

that the self and mutual reactivities of A and U are similar. Cycling at pH 11 increases the yield but does not change significantly the product distribution. At pH 10, instead, cycle 1 and cycle 10 are markedly different, initially dominated by homo-nucleotide products, slightly favoring A-rich products over U-rich ones, and later compensated by a larger growth of hetero-nucleotide polymerization events. This suggests that the molecular arrangement in the dry state could be affected by the presence of short oligomers in the preceding fluid solution.

GC mixtures were instead characterized by a strong difference of polymerization yields for individual G and C systems (**Fig. 3a** and **S17**), which decreases only for pH ≥ 11 or large n, and by ISO-CRY phase separation, at each pH and n (**Fig. S18**). The distribution of oligomers produced in wet-dry cycles of CG mixtures were indeed found to be dominated by poly-G sequences, due to the larger reactivity of G, as apparent in **Fig. 4b (**see also **Fig. S23)**. As expected from the yield measurements (**Fig. 3a, S17**), this effect was much stronger at pH 10. At this pH, the distribution of products grew in amplitude from cycle 1 to cycle 10, but its uneven character remained. At pH 11 we observed a flatter distribution which became closer to the distribution expected for random polymerization as the number of cycles increased (**Fig. S25**). Inspection of the products revealed that this is the consequence of a minor increase of heterogeneous polymerization and of a significant decrease of the number of poly-G chains longer than 3 nucleotides (arrows). Such a decrease is in line with the reduced yield in G solutions upon cycling at pH 11 (**Fig. 3a**) and with the cleavage of longer poly-G when cycles were performed in a controlled highly alkaline environment (**Fig. S15**). The dominance of poly-G chains suggested that a residual phase separation due to the self-assembly propensity of G was still present at each pH and n, making the physical proximity of C and G less likely, in agreement with PTOM observations (**Fig. S18**).

The products distribution in AUGC mixture (**Fig. 4c**) appeared to be a combination of those of the two binary mixtures. At pH 10 the inclusion of all the four nucleotides was found to be uneven throughout all cycles, in agreement with the larger reactivity of G (**Fig. 3a** and **S17**), and mixed products including G (e.g. GCC, GAA and GUU) tended to have lower concentration than mixed products without G (e.g., CAA, CUU and AUU), in line with the presence of phase separation (**Fig. 3c**). At pH 11, we observed a rather flat base sequence distribution in short oligomers (**Fig. S24**), which correlates with the expected decrease in the reactivity difference between G and the other nucleobases (**Fig. S17**), the enhanced cleavage of long poly-G (**SI Fig. S13**) and the suppression of phase separation (**Fig. 3c**) upon cycling. This reshuffling mechanism, driven by a combination of oligomer growth, via residual cyclic-phosphate transesterification, and oligomer breakdown, through hydrolysis reactions (**SI Fig. S21**), led to a stable production of well-mixed short oligomers after 10 wet-dry cycles, indicating a possible self-regulating pathway for the prebiotic production of randomized RNA oligomers with all four nucleobases.

At pH 12, the sequence distributions of products for AU, GC, and AUGC exhibited an even closer alignment with the expected distribution for random polymerization (**Fig. S25-26**). This observation is consistent with the more uniform reactivity among the nucleotide species under these conditions (**Fig. S17**). However, the oligomer lengths were significantly constrained due to increased hydrolysis at high pH (**Fig. S19-21**).

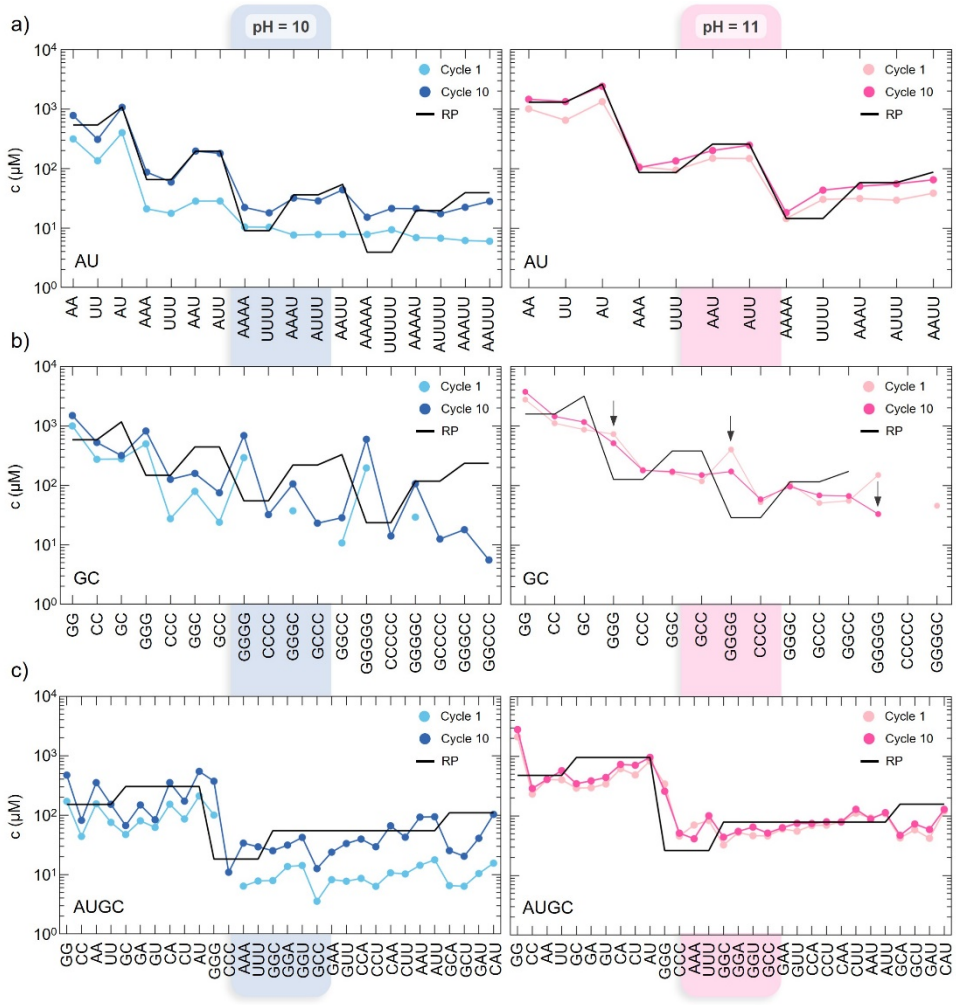

Fig. 4: HPLC-MS analysis of nucleobases composition for products formed in mixtures.
a) Composition distribution of all the detected oligomers in AU mixtures after the 1st and 10th dehydration cycle at pH 10 (left panel) and pH 11 (right panel). Black line represents the expected distribution in the case of random polymerization (RP). b) Same as panel a for GC mixtures. Arrows mark the oligo-G sequences whose population is reduced by cycling because of hydrolysis. c) Same as panel a for AUGC mixtures. In the panels the enumeration of sequences has been limited to length 4 or 5 (a and b) and to length 3 (c) for clarity.

Conclusions

We showed evidence that the long-standing problem of the abiotic polymerization of RNA in prebiotically plausible conditions can be approached by the unassisted polymerization of 2',3'-cNMPs prepared at mM concentration in salt-poor aqueous solutions that undergo periodic dehydration and hydration at room temperature. Polymerization occurred in mild alkaline pH conditions without added catalysts, external activators or further added prebiotically chemistry that would reduce its probability. Alkaline conditions are found even today in the surface waters of volcanic islands [43] and alkaline lakes [44] and likely would have been found similarly on prebiotic Earth. Such a setting would also implement a wet-dry cycle by day-night cycles as well as differences of weather conditions.

We found large polymerization yields and a broad variety of RNA sequences containing all four nucleotides. We interpreted the larger reactivity of G as a consequence of its natural propensity to self-assemble into ordered G-quadruplex columns. Once these structures were destabilized by pH

or G-quartet adverse ions such as Li^+, the reactivity of G significantly lowered, enabling to equalize the reactivity among nucleobases.

Different combinations of pH and cycling process were sufficient to create a nascent RNA population in equimolar solutions of the four nucleotides, with alkaline pH (8–10) favoring longer, G-dominated oligomers and more alkaline conditions (pH = 11–12) promoting shorter, more compositionally diverse sequences (**Fig. S26**). We found that a pH 11 gave an optimal trade-off, with a 36% yield reached after 4 dry-wet cycles in AUGC mixtures and detecting 6-mer RNA oligomers at 10 μM concentration (**Fig. S21**). Under these conditions, the compositional diversity in terms of nucleobase sequence in the polymerized RNA chains is favored. The reported polymerization of RNA under dry-wet cycles provides a solid basis for the starting of early RNA evolution [45]. Supplementary alternation of diluted-phase reshuffling and concentrate-phase self-assembly [46], together with the regeneration of 2',3'-cyclic phosphate termini [9], could lead to the transition to mechanisms of non-enzymatic oligomers polymerization [34,35] and templated ligation [42], promoting the further elongation and information copying of the short random-sequence RNA population here obtained.

Materials and Methods

Materials

2',3'-cyclic phosphate (2'3'-cNMPs), 2'-phosphate (2'-NMPs) and 3'-phosphate (3'-NMPs) nucleotides were purchased from BioLog (Germany) in their sodium salt form. Oligonucleotides were purchased from Biomers (Germany) and chemicals from Merck (Germany).

Stock solutions and samples preparation

Diluted solutions (~10 mM) of single 2'3'-cNMPs species (cAMP, cUMP, cGMP, cCMP) and equimolar binary and quaternary mixtures (AU, GC, AUGC) were prepared in MilliQ water (Millipore), portioned in 200 µL plastic tubes (Eppendorf), corresponding to1 µmol of nucleotides in each tube, and then lyophilized overnight. The resulting powders were stored at room temperature. Samples were prepared resuspending each portion in 20 µL of MilliQ water to achieve the initial concentration c_0 = 50 mM and the pH was adjusted using potassium hydroxide (KOH). Solutions were evaporated into a flat glass-bottom multi-well plate (Corning) in open air at room temperature over 24 hours. On average all samples achieved the dry state within 8 – 10 hours. Evaporations of 2 µL solutions were also performed on a glass microscopy slide. In this case, due to the lower volume and the open geometry, the evaporation was faster (10 to 20 minutes) but the oligomerization yields were found to be similar. Measurements of the concentration during evaporation were performed by weighing 20 µL of 2'3'-cNMPs solutions in a plastic tube (Eppendorf), over time, with a scale with 0.01 mg sensitivity (ABT 100-5M from Kern).

Ion exchange

Contrarily to K^+, the affinity of Li^+ ions for G-quadruplexes has been reported to be lower than that of Na^+ [24]. Therefore, complete replacement of Na^+ counterions with Li^+ ions was needed to probe the effect of Li^+ ions. This was done through the following ion-exchange protocol. 600 mg of resin (Dowex 50WX8 hydrogen form) were placed in a 2 mL plastic tube (Eppendorf) together with 1 mL of 2 M solution of LiOH and stirred with a magnetic stirrer. After 5h, if pH was < 7, the supernatant was replaced with fresh 2M LiOH and the solution was further stirred for 5h. The Li^+ enriched resin was filtered and loaded in a 1 mL syringe. 300 µL of a 30 mM solution of cyclic nucleotides was loaded on top of the resin, eluted and collected in 2 mL plastic tube. The resin was further washed with 1 mL of MilliQ water and collected in the same tube. The obtained solution was promptly flash-frozen and lyophilized. The replacement of Na^+ with K^+, following the same procedure, didn't produce different behavior compared to the direct addition of KOH to sodium salt cNMPs.

Microscopy observation

Brightfield and polarized transmitted optical microscopy observations were performed with an inverted optical microscope (TE200 from Nikon, Japan), equipped with 4x, 10x, 20x and 50x magnification objectives. Images were acquired with a Nikon DS-Fi3 CMOS color camera, controlled by NIS-Elements BR software (version 5.11.03).

Dry-wet cycles protocol

Samples were rehydrated to c_0 = 50 mM every 24 hours by adding deionized water and without any pH adjustment. After each cycle, 0.3 µL of rehydrated solutions were collected for pH measurement

with pH-indicator strips (Merck) and 0.7 µL were collected for HPLC analysis. All experiments were performed in 2 independent replicas.

HPLC analysis

High-performance liquid chromatography (HPLC) analyses were performed with a WaveTransgenomic (Hitachi) instrument equipped with a Xbridge BEH C18 OST column (4.6x50 mm, particles size = 2.5 µm) and a deuterium lamp (Hitachi, 892-2550). The instrument was calibrated with a ladder of oligomers for each nucleotide species (3'-phosphate ending 1mer, 2mer, 4mer and 10mer). 100% TEAA (bottle A) and 75% TEAA 25% acetonitrile (bottle B) were used as solvents. Each extracted reaction sample was diluted to 1 mM final concentration with MilliQ water. Then, 10 nmol of nucleotides (10 µL) were injected into the HPLC column previously equilibrated at 65°C. Once the temperature was stable, the flowrate was set at 1 mL/min and the following step gradient was performed: 100% A for 3 min, 0% to 60% B in 15 min, 50% to 46% B in 2 min, 46% to 0% B in 1 min. UV absorbance was measured at λ = 260 nm. See Supplementary Methods for chromatogram analysis.

LC-MS acquisition method

The samples were received in lyophilized state and then rehydrated in RNAse-free water (Thermo Fisher Scientific). 10 nmol (for individual nucleotide samples) to 40 nmol (for cAUGC samples) were injected in the HPLC for analysis, without further treatment for the majority of the samples.
Measurements were performed on a HPLC (Agilent 1260 Infinity II) coupled to an electrospray ionization time-of-flight (ESI-TOF) mass spectrometer (Agilent 6230B with dual AJS EIS). The column used was an Agilent Advance Oligonucleotide C18 Column (4.6 x 150mm 2.7-Micron) heated at 60°C and the oligomers were separated by length ion-pairing reverse-phase HPLC. The eluent consisted of mixes of water (Bottle A) and methanol (Bottle B: 50% water, 50% methanol) containing each trimethylamine (TEA) and 8 mM hexafluoroisopropanol (HFIP), with a gradient elution at a flow of 1 mL/min. The method started with 1% of B for 5 minutes, followed by a gradient, increasing from 1% to 30% B over 22.5 minutes and then to 40% for 15 minutes. Then, the column was flushed with 100% B for 5 minutes before being returned to 1% for 6 minutes, to re-equilibrate the column.
Detection of eluted mononucleotides and oligonucleotides was achieved using ESI-TOF in negative mode (employing specific source parameters: Gas temperature: 325°C, Drying gas flow: 13 l/min, Sheath gas temperature: 400°C, Sheath gas flow: 12 l/min, VCap: 3500 V, Nozzle Voltage: 2000V) and Diode Array Detector (DAD) WR (wavelength used: 260.4 nm).

Acknowledgments

Authors would like to thank Saroj K. Rout, Matt Glaser and Gregory P. Smith for useful discussions. F.C. acknowledges support by Fondazione Cariplo, grant Young Researcher n° 2023-1095. TB acknowledges support from Ministero dell'Università e della Ricerca (MUR): NextGenerationEU (PNRR M4C2 - Investimento 1.4-CN00000041-PNRR_CN3RNA_SPOKE9). T.P.F acknowledges support from Ministero dell'Università e della Ricerca (MUR), PRIN2022, grant n° 2022H7MH23; University of Milan, Piano di Sostegno alla Ricerca, PSR-2023 and PSR-2024. D.B. acknowledges support from German Research Foundation (DFG) - CRC 392 Molecular Evolution in Prebiotic– Project-ID 521256690 and Excellence Cluster ORIGINS under Germany's Excellence Strategy EXC-2094-390783311; Simons Foundation, grant number 327125; European Research Council, ERC-2017-ADG, EvoTrap #787356, Center for NanoScience (CeNS).

Conflict of Interest

The authors declare no conflict of interest.

Author Contributions

T.B., D.B., and T.P.F. conceived the research; F.C., F.F. and T.P.F. designed the experiments; F.C., J.L., F.F. and S.W. performed the experiments; F.C., F.F. and J.L. analyzed the data; F.C., F.F., T.B. and T.P.F. wrote the manuscript draft; all authors edited and reviewed the manuscript final version.

References

1. Gilbert, W. The RNA World. *Nature* **1986**, *319*, 618, doi:10.1038/319618a0.
2. Joyce, G.F. The Antiquity of RNA-Based Evolution. *Nature* **2002**, *418*, 214–221.
3. Whitaker, D.; Powner, M.W. On the Aqueous Origins of the Condensation Polymers of Life. *Nat. Rev. Chem.* **2024**, *8*, 817–832, doi:10.1038/s41570-024-00648-5.
4. Motsch, S.; Tremmel, P.; Richert, C. Regioselective Formation of Rna Strands in the Absence of Magnesium Ions. *Nucleic Acids Res.* **2020**, *48*, 1097–1107, doi:10.1093/NAR/GKZ1125.
5. Ferris, J.P.; Ertem, G. Oligomerization of Ribonucleotides on Montmorillonite: Reaction of the 5'-Phosphorimidazolide of Adenosine. *Science (80-.).* **1992**, *257*, 1387–1389, doi:10.1126/science.1529338.
6. Sawai, H.; Orgel, L.E. Oligonucleotide Synthesis Catalyzed by the Zinc(2+) Ion. *J. Am. Chem. Soc.* **1975**, *97*, 3532–3533, doi:10.1021/ja00845a050.
7. Sawai, H. Catalysis of Internucleotide Bond Formation by Divalent Metal Ions. *J. Am. Chem. Soc.* **1976**, *98*, 7037–7039, doi:10.1021/ja00438a050.
8. Powner, M.W.; Gerland, B.; Sutherland, J.D. Synthesis of Activated Pyrimidine Ribonucleotides in Prebiotically Plausible Conditions. *Nature* **2009**, *459*, 239–242, doi:10.1038/nature08013.
9. Gibard, C.; Bhowmik, S.; Karki, M.; Kim, E.K.; Krishnamurthy, R. Phosphorylation, Oligomerization and Self-Assembly in Water under Potential Prebiotic Conditions. *Nat. Chem.* **2018**, *10*, 212–217, doi:10.1038/nchem.2878.
10. Lipkin, D.; Talbert, P.T.; Cohn, M. The Mechanism of the Alkaline Hydrolysis of Ribonucleic Acids. *J. Am. Chem. Soc.* **1954**, *76*, 2871–2872, doi:10.1021/ja01640a004.
11. Verlander, M.S.; Lohrmann, R.; Orgel, L.E. Catalysts for the Self-Polymerization of Adenosine Cyclic 2′,3′-Phosphate. *J. Mol. Evol.* **1973**, *2*, 303–316, doi:10.1007/BF01654098.
12. Verlander, M.S.; Orgel, L.E. Analysis of High Molecular Weight Material from the Polymerization of Adenosine Cyclic 2′, 3′-Phosphate. *J. Mol. Evol.* **1974**, *3*, 115–120, doi:10.1007/BF01796557.
13. Dass, A.V.; Wunnava, S.; Langlais, J.; von der Esch, B.; Krusche, M.; Ufer, L.; Chrisam, N.; Dubini, R.C.A.; Gartner, F.; Angerpointner, S.; et al. RNA Oligomerisation without Added Catalyst from 2′,3′-Cyclic Nucleotides by Drying at Air-Water Interfaces. *ChemSystemsChem* **2022**, *5*, 1–9, doi:10.1002/syst.202200026.
14. Rout, S.K.; Wunnava, S.; Powner, M.; Sponer, J.E.; Mast, C.B.; Braun, D. Amino Acids Catalyze RNA Formation under Ambient Alkaline Conditions. *Res. Sq. Prepr.* **2024**, 0–12, doi:doi.org/10.21203/rs.3.rs-4343389/v1.
15. Becker, S.; Schneider, C.; Okamura, H.; Crisp, A.; Amatov, T.; Dejmek, M.; Carell, T. Wet-Dry Cycles Enable the Parallel Origin of Canonical and Non-Canonical Nucleosides by Continuous Synthesis. *Nat. Commun.* **2018**, *9*, 1–9, doi:10.1038/s41467-017-02639-1.
16. Campbell, T.D.; Febrian, R.; McCarthy, J.T.; Kleinschmidt, H.E.; Forsythe, J.G.; Bracher, P.J. Prebiotic Condensation through Wet–Dry Cycling Regulated by Deliquescence. *Nat. Commun.* **2019**, *10*, doi:10.1038/s41467-019-11834-1.
17. Forsythe, J.G.; Yu, S.S.; Mamajanov, I.; Grover, M.A.; Krishnamurthy, R.; Fernández, F.M.; Hud, N. V. Ester-Mediated Amide Bond Formation Driven by Wet-Dry Cycles: A Possible Path to Polypeptides on the Prebiotic Earth. *Angew. Chemie - Int. Ed.* **2015**, *54*, 9871–9875, doi:10.1002/anie.201503792.
18. Ross, D.; Deamer, D. Dry/Wet Cycling and the Thermodynamics and Kinetics of Prebiotic Polymer Synthesis. *Life* **2016**, *6*, 28, doi:10.3390/life6030028.
19. Higgs, P.G. The Effect of Limited Diffusion and Wet–Dry Cycling on Reversible Polymerization Reactions: Implications for Prebiotic Synthesis of Nucleic Acids. *Life* **2016**, *6*, doi:10.3390/life6020024.
20. Ianeselli, A.; Salditt, A.; Mast, C.; Ercolano, B.; Kufner, C.L.; Scheu, B.; Braun, D. Physical Non-Equilibria for Prebiotic Nucleic Acid Chemistry. *Nat. Rev. Phys.* **2023**, *5*, 185–195, doi:10.1038/s42254-022-00550-3.
21. Jia, T.Z.; Chandru, K.; Hongo, Y.; Afrin, R.; Usui, T.; Myojo, K. Membraneless Polyester

Microdroplets as Primordial Compartments at the Origins of Life. *Proc. Natl. Acad. Sci. U. S. A.* **2019**, *116*, 15830–15835, doi:10.1073/pnas.1902336116.
22. Fares, H.M.; Marras, A.E.; Ting, J.M.; Tirrell, M. V.; Keating, C.D. Impact of Wet-Dry Cycling on the Phase Behavior and Compartmentalization Properties of Complex Coacervates. *Nat. Commun.* **2020**, *11*, doi:10.1038/s41467-020-19184-z.
23. Pearce, B.K.D.; Pudritz, R.E.; Semenov, D.A.; Henning, T.K. Origin of the RNA World: The Fate of Nucleobases in Warm Little Ponds. *Proc. Natl. Acad. Sci.* **2017**, *114*, 11327–11332, doi:10.1073/pnas.1710339114.
24. Davis, J.T. G-Quartets 40 Years Later: From 5'-GMP to Molecular Biology and Supramolecular Chemistry. *Angew. Chemie - Int. Ed.* **2004**, *43*, 668–698, doi:10.1002/anie.200300589.
25. Mariani, P.; Mazabard, C.; Garbesi, A.; Spada, G.P. A Study of the Structure of the Lyomesophases Formed by the Dinucleoside Phosphate d(GpG). An Approach by x-Ray Diffraction and Optical Microscopy. *J. Am. Chem. Soc.* **1989**, *111*, 6369–6373, doi:10.1021/ja00198a057.
26. Gottarelli, G.; Proni, G.; Spada, G.P. The Self-Assembly and Lyotropic Mesomorphism of Riboguanylic Acids (GMP). *Liq. Cryst.* **1997**, *22*, 563–566, doi:10.1080/026782997208956.
27. Engelhart, A.E.; Powner, M.W.; Szostak, J.W. Functional RNAs Exhibit Tolerance for Non-Heritable 2'-5' versus 3'-5' Backbone Heterogeneity. *Nat. Chem.* **2013**, *5*, 390–394, doi:10.1038/nchem.1623.
28. Kanavarioti, A.; Monnard, P.-A.; Deamer, D.W. Eutectic Phases in Ice Facilitate Nonenzymatic Nucleic Acid Synthesis. *Astrobiology* **2001**, *1*, 271–281, doi:10.1089/15311070152757465.
29. Flory, J. Molecular Size Distribution in Linear Condensation Polymers. *J. Am. Chem. Soc.* **1936**, *1*, 1877–1885.
30. Smulders, M.M.J.; Nieuwenhuizen, M.M.L.; De Greef, T.F. a; Van Der Schoot, P.; Schenning, a. P.H.J.; Meijer, E.W. How to Distinguish Isodesmic from Cooperative Supramolecular Polymerisation. *Chem. - A Eur. J.* **2010**, *16*, 362–367, doi:10.1002/chem.200902415.
31. Jones, E.L.; Mlotkowski, A.J.; Hebert, S.P.; Schlegel, H.B.; Chow, C.S. Calculations of PKa Values for a Series of Naturally Occurring Modified Nucleobases. *J. Phys. Chem. A* **2022**, *126*, 1518–1529, doi:10.1021/acs.jpca.1c10905.
32. Lydon, J. Chromonic Review. *J. Mater. Chem.* **2010**, *20*, 10071–10099, doi:10.1039/b926374h.
33. Smith, G.P.; Fraccia, T.P.; Todisco, M.; Zanchetta, G.; Zhu, C.; Hayden, E.; Bellini, T.; Clark, N.A. Backbone-Free Duplex-Stacked Monomer Nucleic Acids Exhibiting Watson – Crick Selectivity. *Proc. Natl. Acad. Sci. U. S. A.* **2018**, *115*, E7658–E7664, doi:10.1073/pnas.1721369115.
34. Fraccia, T.P.; Smith, G.P.; Zanchetta, G.; Paraboschi, E.; Yi, Y.; Walba, D.M.; Dieci, G.; Clark, N.A.; Bellini, T. Abiotic Ligation of DNA Oligomers Templated by Their Liquid Crystal Ordering. *Nat. Commun.* **2015**, *6*, 12864, doi:10.1038/ncomms7424.
35. Todisco, M.; Fraccia, T.P.; Smith, G.P.; Corno, A.; Bethge, L.; Klussmann, S.; Paraboschi, E.M.; Asselta, R.; Colombo, D.; Zanchetta, G.; et al. Nonenzymatic Polymerization into Long Linear RNA Templated by Liquid Crystal Self-Assembly. *ACS Nano* **2018**, doi:10.1021/acsnano.8b05821.
36. Yan, Y.Y.; Tan, J.H.; Lu, Y.J.; Yan, S.C.; Wong, K.Y.; Li, D.; Gu, L.Q.; Huang, Z.S. G-Quadruplex Conformational Change Driven by PH Variation with Potential Application as a Nanoswitch. *Biochim. Biophys. Acta - Gen. Subj.* **2013**, *1830*, 4935–4942, doi:10.1016/j.bbagen.2013.06.019.
37. Lane, A.N.; Chaires, J.B.; Gray, R.D.; Trent, J.O. Stability and Kinetics of G-Quadruplex Structures. *Nucleic Acids Res.* **2008**, *36*, 5482–5515, doi:10.1093/nar/gkn517.
38. Baldassarri, E.J.; Ortore, M.G.; Spinozzi, F.; Round, A.; Ferrero, C.; Mariani, P. K+ vs. Na+ Effects on the Self-Assembly of Guanosine 5'-Monophosphate: A Solution SAXS Structural Study. *Nanomaterials* **2020**, *10*, 1–20, doi:10.3390/nano10040629.
39. Pinnavaia, T.J.; Marshall, C.L.; Mettler, C.M.; Fisk, C.L.; Miles, H.T.; Becker, E.D. Alkali Metal Ion Specificity in the Solution Ordering of a Nucleotide, 5'-Guanosine Monophosphate.

J. Am. Chem. Soc. **1978**, *100*, 3625–3627, doi:10.1021/ja00479a070.
40. Fraccia, T.P.; Martin, N. Non-Enzymatic Oligonucleotide Ligation in Coacervate Protocells Sustains Compartment-Content Coupling. *Nat. Commun.* **2023**, *14*, 1–12, doi:10.1038/s41467-023-38163-8.
41. von Kiedrowski, G. A Self-Replicating Hexadeoxynucleotide. *Angew. Chem., Int. Ed. Engl.* **1986**, *25*, 932–935.
42. Calaça Serrão, A.; Wunnava, S.; Dass, A. V.; Ufer, L.; Schwintek, P.; Mast, C.B.; Braun, D. High-Fidelity RNA Copying via 2′,3′-Cyclic Phosphate Ligation. *J. Am. Chem. Soc.* **2024**, *146*, 8887–8894, doi:10.1021/jacs.3c10813.
43. Arnórsson, S. Geothermal Systems in Iceland: Structure and Conceptual Models—I. High-Temperature Areas. *Geothermics* **1995**, *24*, 561–602, doi:https://doi.org/10.1016/0375-6505(95)00025-9.
44. Garrels, R.M.; Mackenzie, F.T. Origin of the Chemical Compositions of Some Springs and Lakes. In *Equilibrium Concepts in Natural Water Systems*; Advances in Chemistry; AMERICAN CHEMICAL SOCIETY, 1967; Vol. 67, pp. 10–222 ISBN 9780841200685.
45. Gilbert, W. Origin of Life: The RNA World. *Nature* **1986**, *319*, 618.
46. Marni, S.; Fraccia, T.P.; Bellini, T. Random-Sequence DNA Oligomers Make Liquid Crystals: A Case of Collective Ordering in a Superdiverse Environment. *ACS Nano* **2024**, *18*, 34034–34043, doi:10.1021/acsnano.4c09400.